



Development of Mathematical Model for Percentage of Elongation of TIG Welded Duplex Stainless Steel

Sandip Mondal ^{1,*}, Goutam Nandi ², Pradip Kumar Pal ²



¹ Department of Mechanical Engineering, Haldia Institute of Technology, Haldia-721657, India

² Department of Mechanical Engineering, Jadavpur University, Kolkata-700032, India

*Corresponding authors email: sandip_mondal2004@rediffmail.com

DOI: <https://doi.org/10.54392/irjmt2221>

Received: 11-01-2022; Revised: 03-02-2022; Accepted: 03-02-2022; Published: 05-02-2022

Abstract: Quality strongly depends on good mechanical properties of any manufacturing material. Similarly, quality of Tungsten Inert Gas (TIG) welding of Duplex Stainless Steel (DSS) depends on good mechanical properties like percentage of elongation, ultimate tensile strength etc. Better Percentage of Elongation (PE) is produced using proper welding parameters and their values at the time of TIG welding. In this study, TIG welding has been done on ASTM/UNS 2205 duplex stainless steel materials. A new mathematical model is developed using non-linear regression analysis for the prediction of percentage of elongation. The variables used in the prediction models are selected welding parameters like welding current, gas flow rate and speed of welding. A residual plot for PE has been developed to validate the mathematical model. Calculation of percentage deviation for PE has been made. Comparison of measured and predicted PE value has been done by graphical representation. The relationship between percentage of elongation and the welding parameters has been illustrated graphically by surface plots and contour plots as well. Combined effects of any pair of input parameters on PE are represented graphically with the help of three-dimensional surface plots. According to this analysis, the models provide good PE with the data used in this study.

Keywords: Duplex stainless steel, Mathematical modeling, Percentage of elongation, Tungsten inert gas welding

1. Introduction

Duplex Stainless Steel (DSS) is made by exceptional blend of double phase configuration of ferrite with austenite. 50% ferritic and 50% austenitic phase structure has generally been observed in grain configuration of DSS. It has got high yield strength, good ductility, ability to withstand high working temperature and good corrosion resistance. Application of DSS is increasing day to day due to the favorable weldability property of duplex stainless steel. Duplex stainless steels are sometimes used as a substitute to Austenitic Stainless Steels (ASS) in different areas of application like reaction vessels and pipelines of chemical, oil refinery and gas industries. Austenite structure provides a unique arrangement of strength. Ferrite phase provides local corrosion resistance.

Murugan *et al.*, [1] prepared a mathematical model for five levels factorial technique. Using this method, bead geometry of welding of 316L stainless steel into IS2062 structural steel had been investigated and illustrated in graphical form. They searched for the selection of appropriate levels of process parameters to reach the desired quality for the welded product. Badji *et*

al., [2] investigated phase structure configuration and different properties of 2205DSS materials. They performed heat treatment on DSS materials by annealing, using temperature 800°C - 1000°C. They showed that the most of ferritic phase structures were positioned around the HAZ zone. Sotomayor *et al.*, [3] determined the adhesive property of duplex stainless steel on a thermoplastic. They also examined the rupture failures of that material. Several conditions like humidity had significant role to evaluate the effectiveness of surface treatment. Palani and Murugan [4] investigated the cladding effect using different parameters such as welding current, welding speed and nozzle-to-plate distance on the weld bead geometry. Del Coz Diaz *et al.*, [5] showed the important role of the material properties in the final deformed shape of two different stainless steels using finite element method including the birth and death technique. They also investigated that opposite angular deformation and longitudinal bending occur when these steels are welded with a similar TIG procedure. Pandya and Menghani [6] prepared a mathematical model for prediction of tensile properties of dissimilar AA6061-T6 to Cu welds. They used friction stir welding process with Zn interlayer. Tarng and Yang [7] applied Taguchi technique to optimize weld pool

structure. Tarnag *et al.*, [8] investigated on the optimal weld bead structure of TIG welded stainless steel to determine the process parameters by using modified Taguchi method. Tarnag *et al.*, [9] researched related to grey-based Taguchi technique to decide optimal process factors of submerged arc welding, concern of various weld properties. Murta *et al.*, [10] developed Mathematical model for predicting mechanical properties in rebar manufacturing. They showed that an artificial neural network can be useful in evaluating and choosing the most adequate parameters to achieve the desired steel properties. Badjia *et al.*, [11] observed as in the received metal the textures of both phases are mixtures of recrystallization textures and deformation, which generally establish between the material of single-phase BCC and FCC structure. Ul-Haq *et al.*, [12] researched on textures and microstructures of duplex stainless steel. They also showed the rolling texture development in the micro-structure of duplex stainless steel.

Literature survey suggests that there is a need of further extensive research in the area of TIG welding of duplex stainless steel. DSS is being extremely used in oil and chemical industry. But the sufficient research work has not been done on this emerging field. In so far as TIG welding of duplex stainless steel is concerned, knowledge-base is not sufficiently rich. More and extensive research may lead to develop a sound knowledge-base which will help better understanding of the various aspects relating to duplex stainless-steel welding. For that reason, mathematical modeling, metallographic characterization, parametric optimization, analysis of joint performance etc. are very much important. Investigation related to these fields will lead to create a strong knowledge-base which will help use of TIG welding in more predictable way with the desired quality of weld.

In the present work, duplex stainless-steel plates are joined by TIG welding. Nine butt-welding joints are made by TIG welding under varied input parameters. The Taguchi's L9 orthogonal array design is used to design the experiments, with three controllable factors, viz. current, welding speed and shielding gas flow rate. Factor levels are chosen on the basis of trial runs and the knowledge of text book. Welding excellence is evaluated by X-ray radiography test. Then, tensile test has been done. A new mathematical model is developed using non-linear regression analysis for the prediction of percentage of elongation. The variables used in the prediction models are selected welding parameters like welding current, gas flow rate and speed of welding. A residual plot for PE has been developed. Calculation of percentage deviation for PE has also been made. Comparison of measured and predicted PE value has been done by graphical representation. The relationship between percentage of elongation and the welding parameters has been illustrated graphically by surface plots and contour plots as well. Combined

effects of any pair of input parameters on PE are represented graphically with the help of three-dimensional surface plots. According to this analysis, the models provide good PE with the data used in this study.

2. Experimental Work

In this experiment, TIG welding was performed on duplex stainless-steel plates. The dimension of each welding pate was taken as 75 mm x 50 mm x 3 mm. Butt welding joint was completed. Filler rod was not utilized at the time of welding process. Argon gas was used as the shielding gas. The diameter of Tungsten electrode was 2.4mm. TIG welding on DSS was completed with the help of IGBT digital welding inverter (400A, III phase) of Electra Engineering (India) Pvt. limited. Materials were welded with suitable welding parameters like current, gas flow rate, welding speed. The photographic view of the arrangement of TIG welding equipment is shown in figure 1. Photographic view of welding sample no. 4 is shown in figure 2. The trial runs of welding joints and final welding joints were completed successfully with the help of these welding equipment.



Figure1. TIG welding setup



Figure 2 Welding sample no. 4

2.1. Base metal

In this study the base metal was a duplex stainless steel (ASTM/UNS: 2205). The chemical composition of this DSS material is shown in table 1. The microstructural feature of the base metal exhibits a duplex structure with embedded grains of austenite and ferrite.

2.2. Process Parameters and their Levels

The process factors were decided based on several experimental trials. Here, 3 levels of current, 3 levels of gas flow rate and 3 levels of welding speed were taken to complete the joining process. Welding process factors with their levels are listed in table 2.

3. Results and Discussion

3.1. Tensile Test and Results

Completing X-ray radiography investigation, tensile testing samples were created from the TIG welding plates, by Electronica sprintcut-734 Wire Electrical Discharge Machining (WEDM) (input power

supply 3 Phase, AC 415 V, 50 Hz, linked load 15 KVA). Photographic view of tensile specimen preparation by WEDM is shown in figure 3(a) Photographic view of tensile test specimens as per ASTM E8 is shown in figure 3(b) and tensile sample after test is shown by figure 3(c).

The tensile testing samples were investigated with the help of tensile testing machine Instron by Blue Star Engineering & Electronics Ltd, Model No.: BSUT-60-JD-SERVO, Serial No.: 2016/048, Maximum Capacity: 600 kN. Data related to percentage of elongation are listed in table 3. These results were used for preparing the mathematical model which was very much necessary to realize the desire excellence of TIG weld within the experimental domain.

Table 1. Composition of DSS

Composition of elements in %	C	Si	Mn	P	S	Cr	Mo	Ni	Al
	0.0210	0.2800	1.7200	0.0220	0.0140	22.6500	3.1800	4.7300	0.0100
	Co	Cu	Nb	Ti	V	Pb	Fe	N	
	0.0780	0.0090	0.0400	0.0080	0.0110	0.0030	67.123	0.1010	

Table 2. Welding process factors with their levels

Factors	Units	Notations	Levels		
			1	2	3
Welding Current	A	C	80	85	90
Gas Flow Rate	l/min	F	7	7.5	8
Welding Speed	mm/s	S	2.3	2.8	3.5



Figure 3 (a) Tensile specimen preparation by WEDM



Figure 3 (b). Tensile test specimen



Figure 3 (c). Tensile sample after test

Table 3. The results of percentage of elongation with welding parameters

Sample No.	Welding Parameter with Value			Percentage of Elongation (%)
	Current (A)	Welding speed (mm/s)	Shielding gas flow rate (l/min)	
1	80	2.3	7	10.4530
2	80	2.8	7.5	11.6650
3	80	3.5	8	17.7770
4	85	2.8	7	14.9470
5	85	3.5	7.5	14.9070
6	85	2.3	8	11.9810
7	90	3.5	7	14.0340
8	90	2.3	7.5	10.9380
9	90	2.8	8	14.4790

4. Regression Analysis of Percentage of Elongation Data (PE)

In this section, Data have been used to generate regression equations, contour and surface plots and to develop and interpret residual plots. The experimentally measured results i.e. actual observations and results obtained through mathematical model i.e. predictions are compared. The analyses have been done for percentage of elongation of TIG welded duplex stainless steel, UNS 2205.

At first, mathematical modeling through non linear regression analysis, of percentage of elongation observations has been made using MINITAB 16 software. Surface plots and contour plots for PE are developed along with residual plots.

4.1. Mathematical Modeling

Percentage of elongation is been expressed in terms of the process variables: welding current (C), gas

flow rate (F) and speed of welding (S) as

$$PE = \theta_1 + \theta_2 (C) + \theta_3 (F) + \theta_4 (S) + \theta_5 (C * F) + \theta_6 (C * S) + \theta_7 (F * S) \quad 1$$

Where θ_1 is the constant coefficient, θ_2 , θ_3 and θ_4 are the coefficients of welding current, gas flow rate and speed of welding respectively.

The final mathematical model to estimate PE is given as

$$PE = 15.3445 + 0.74193 * C - 3.52429 * F - 0.960213 * S - 0.0283667 * C * F - 0.162704 * C * S + 2.44927 * F * S \quad 2$$

Where PE is in %, C is in A, F is in l/min and S is in mm/s.

Gauss-Newton algorithm method is applied to develop this mathematical equation. This equation is prepared keeping maximum iterations 200 and tolerance 0.00001. From θ_1 to θ_7 , starting value for every parameter is 1. The mathematical model is successfully prepared with the help of calculating the estimation of

parameters and correlation matrix for parameter estimates. The parameter estimates and correlation matrix for parameter estimates are given in tables 4 and 5 respectively. Residual plots for PE are also given in figure 4. These residual plots are validating the prepared regression model. From these residual plots it is clearly

observed that maximum data are satisfied and regression model is, therefore, considered valid.

In this analysis, the Sum of Squared Errors (SSE) gets minimized by the set of parameter estimates when the algorithm is converged on the parameter values correctly.

Table 4 Parameter estimates for PE

Parameter	Estimate	SE Estimate	95% CI
Theta1	-15.3445	375.097	(-1629.25, 1598.57)
Theta2	0.7419	5.281	(-21.98, 23.47)
Theta3	-3.5243	61.184	(-266.78, 259.73)
Theta4	-0.9602	124.544	(-536.83, 534.91)
Theta5	-0.0284	0.870	(-3.77, 3.72)
Theta6	-0.1627	0.815	(-3.67, 3.34)
Theta7	2.4493	8.147	(-32.60, 37.50)

Table 5. Correlation matrix for parameter estimates for PE

	Theta1	Theta2	Theta3	Theta4	Theta5	Theta6
Theta2	-0.935479					
Theta3	-0.919549	0.952964				
Theta4	0.276715	0.565030	0.601917			
Theta5	0.833432	0.955626	0.967129	0.760499		
Theta6	0.245371	0.476026	0.604180	0.950949	0.712105	
Theta7	-0.260376	0.582596	0.512188	-0.936752	-0.712105	0.782967

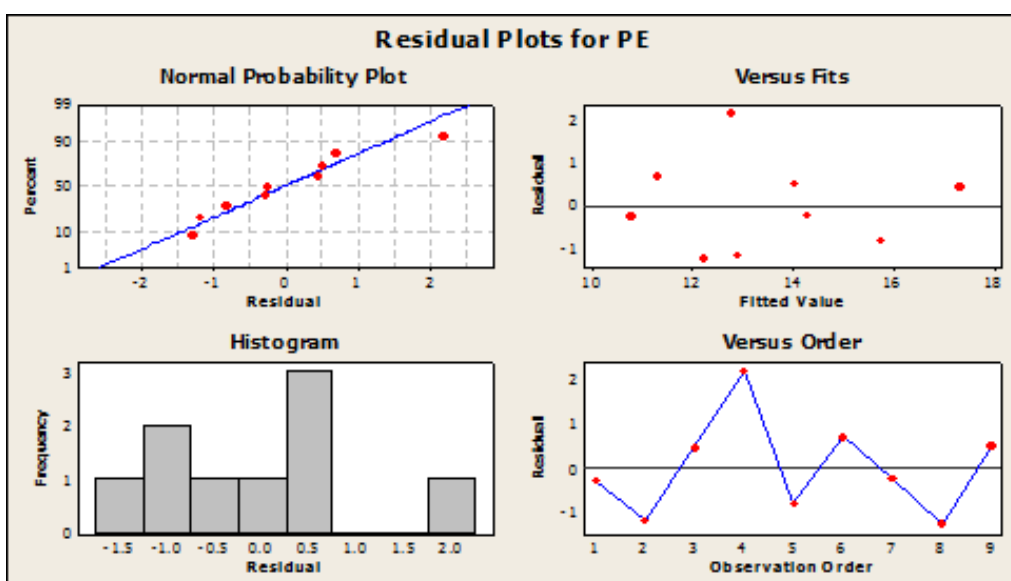


Figure 4. Residual plots for PE

The correct interpretation for each parameter depends on the expectation function and the parameter's place in it. So, the relationship between the predictor and the response has been determined with the help of nonlinear model. The Standard Error of the estimate (SE estimate) is used to measure the precision of the parameter estimate. The smaller standard error describes the more precise estimate. The Confidence Intervals (CI) are ranges of values that are likely to contain the true value of each parameter in the model. The confidence intervals are used to assess the estimate of each parameter estimate. Here, the correlation between parameter estimates is displayed by the correlation matrix. For highly correlated parameter estimates, the number of parameters must be reduced for the simplification of the model.

4.2. Calculation of Percentage Deviation for PE

After generating the mathematical model, it is required to compare between experimentally measured results and results obtained through mathematical

model. This comparison or accuracy of the model has been presented by percentage deviation and graphical plots, are given in table 6 and figure 5 respectively.

Table 6 and figure 5 give percentage deviation and comparison between predictions and actual, which put fair confidence in the mathematical model for percentage of elongation.

The result of percentage deviation for PE and Figure 5 indicate that the mathematical model works satisfactorily for the prediction of the response within the range of the experimental domain.

4.3. Surface Plots and Contour Plots for PE

The relationship between percentage of elongation and the welding parameters has been illustrated graphically by surface plots and contour plots. Combined effects of welding process parameters on any pair of input parameters on PE are represented graphically with the help of three-dimensional surface plots.

Table 6 Calculation of percentage deviation for PE

Sample no.	Experimental result for PE (measured result) in %	Result for PE obtained through mathematical model (prediction result) in %	Percentage of deviation in %
1	10.4530	10.7417	-2.76189
2	11.6650	12.8581	-10.228
3	17.7770	17.3226	2.556112
4	14.9470	12.7649	14.59892
5	14.9070	15.7318	-5.53297
6	11.9810	11.2853	5.806694
7	14.0340	14.2829	-1.77355
8	10.9380	12.2112	-11.6402
9	14.4790	13.9845	3.415291

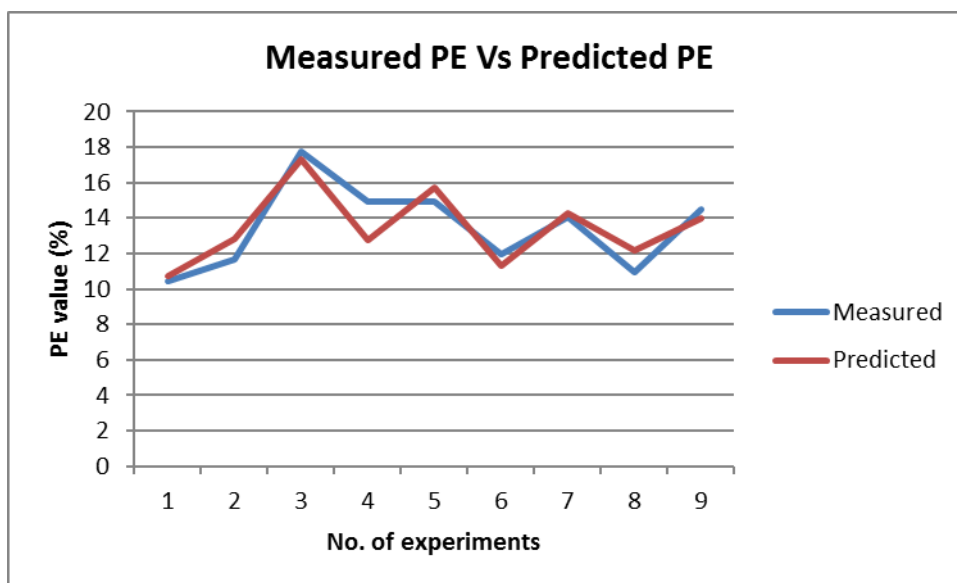


Figure 5. Comparison of measured and predicted PE value

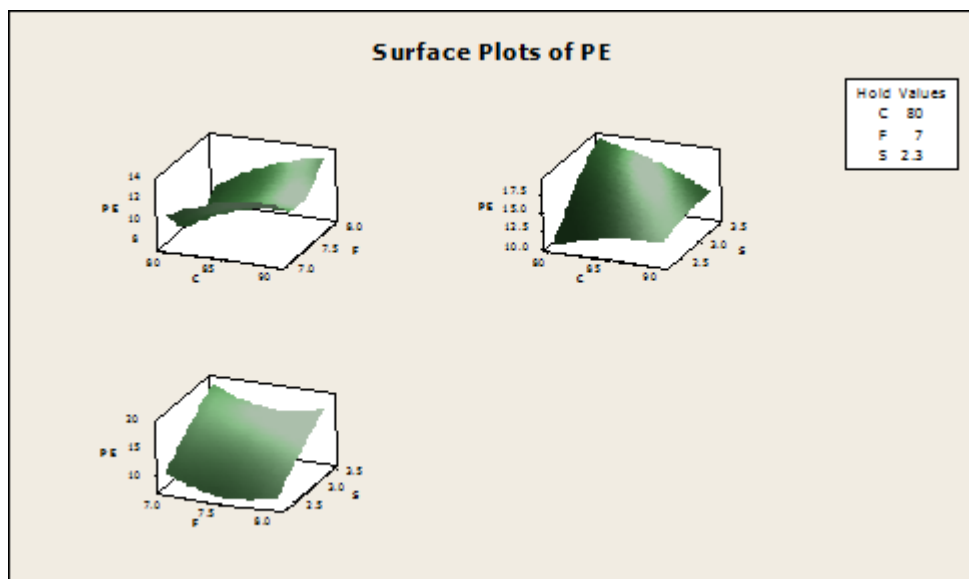


Figure 6 Surface plots of PE when welding current (C), gas flow rate (F) and speed of welding (S) constant at lowest level

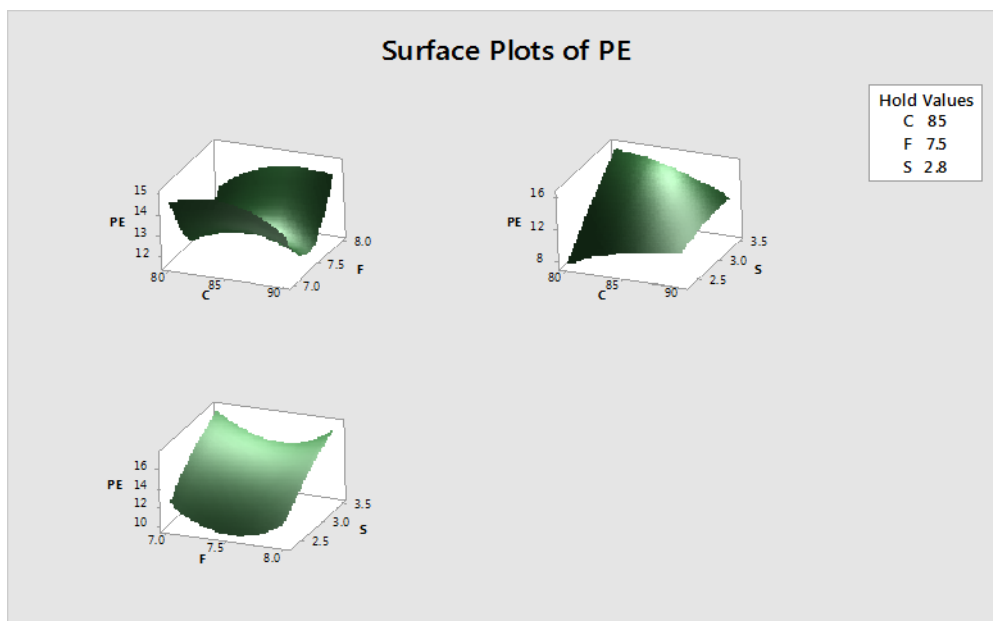


Figure 7. Surface plots of PE when welding current (C), gas flow rate (F) and speed of welding (S) constant at middle level

In surface plots, a response is plotted against any two input variables when the other variable, the third one, is held constant. The contour plots are two-dimensional graphs that show contours of constant response, with the axis system being a specific pair of the process variables, while the other variable is held constant. The plots are particularly necessary when the stationary point is a saddle point or is remote from the design region. But it should be kept in mind that the contour plots are only estimator, they are not generated by deterministic equations. Every point on a contour has a standard error. Interaction effects of the input process parameters on the response(s) are also identified with the help of these plots. The surface plots are shown in

figures 6 – 8 and contour plots are shown in figures 9– 11.

Response surface plots show the combined effect of any two input process factors on the selected responses when the third parameter is held constant position. If the response surface exhibits appreciable bend, curvature or undulation, then interaction effect is considered to be significant. No or very little bend/curvature or undulation of response surface plots leads to the fact that interaction effect is less or insignificant. In figure 6, 7 and 8, less bend or curvature surface plots has been clearly observed when speed of welding is in held position, medium bend or curvature surface plots has been observed when welding current is in held position and higher bend or curvature surface

plots has been observed when gas flow rate is in held position. Here, interaction effects between gas flow rate and welding current with PE revealed less significant than the interaction effects of other combination of two process parameters like gas flow rate and speed of welding with PE, current and speed of welding with PE. This means interaction among the welding factors, welding current (C) and gas flow rate (F) causes lesser influence on the response PE as compared to the interactions among the factors gas flow rate (F), speed of welding (S) and welding current (C), speed of welding (S).

Contour plots (shown in figures 9 – 11) are helpful for estimating the combined effects of any two

parameters on the response. Each line in the plots is a constant - response line. These plots can be utilized almost in the same manner as discussed in the context of response surface plots. The contour lines, with little or no curvature indicate lesser or no interaction effect; whereas bent or circular contours suggest interaction effect to be significant on the response. For example, interaction among the factors welding current (C) and speed of welding (S) is found to be significant in so far as the effect of this interaction on PE is concerned. Interaction effect of welding current (C) and gas flow rate (F) on PE is not so much significant, as revealed in figures 9 – 11, while speed of welding (S) is kept in constant position. All other surface and contour plots can be evaluated in the same manner.

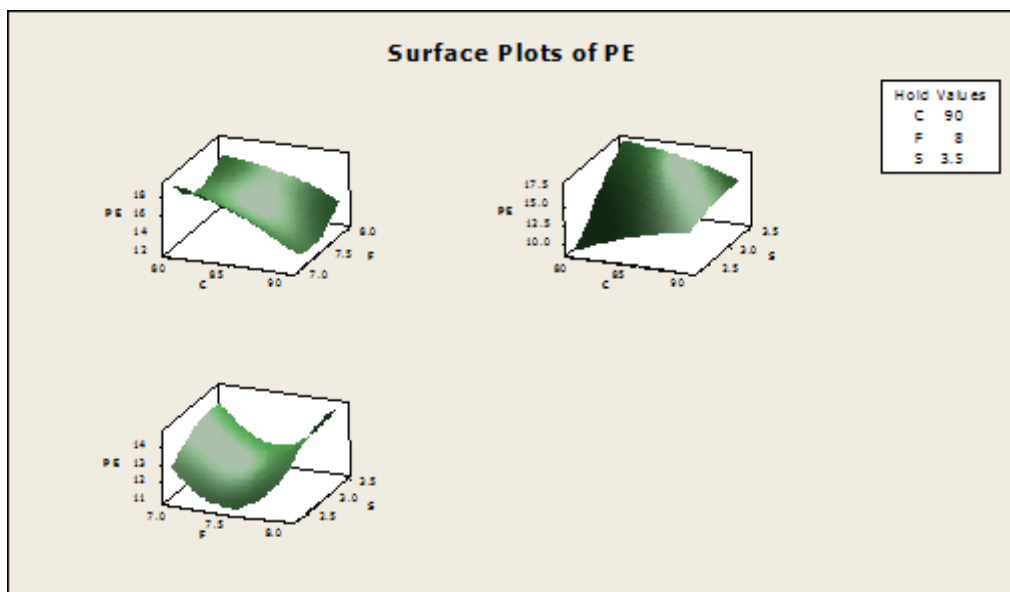


Figure 8. Surface plots of PE when welding current (C), gas flow rate (F) and speed of welding (S) constant at highest level

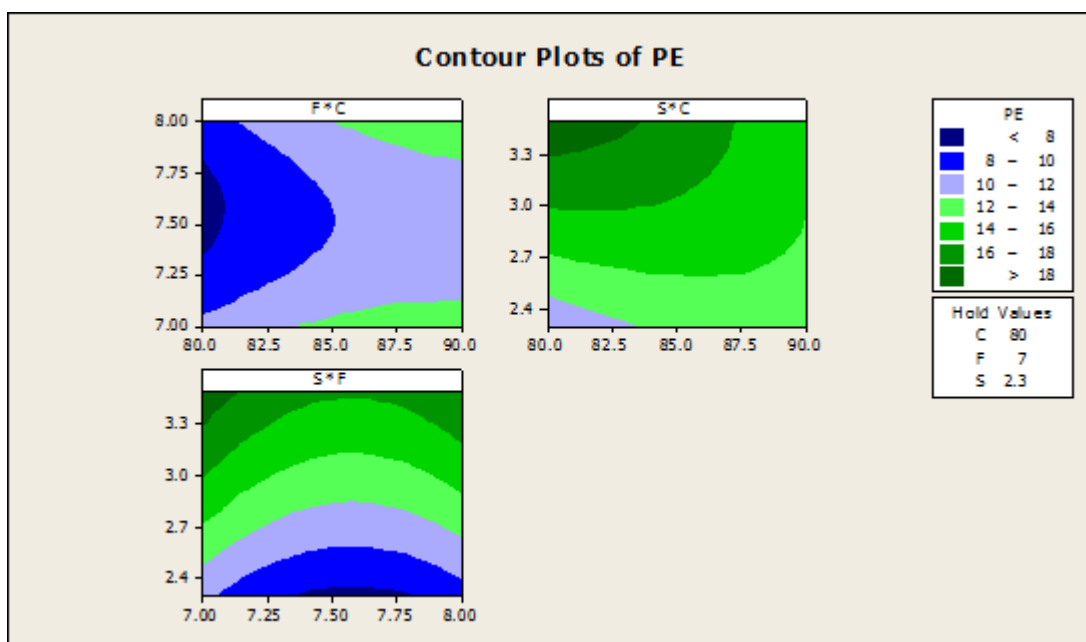


Figure 9. Contour plots of PE when welding current (C), gas flow rate (F) and speed of welding (S) constant at lowest level

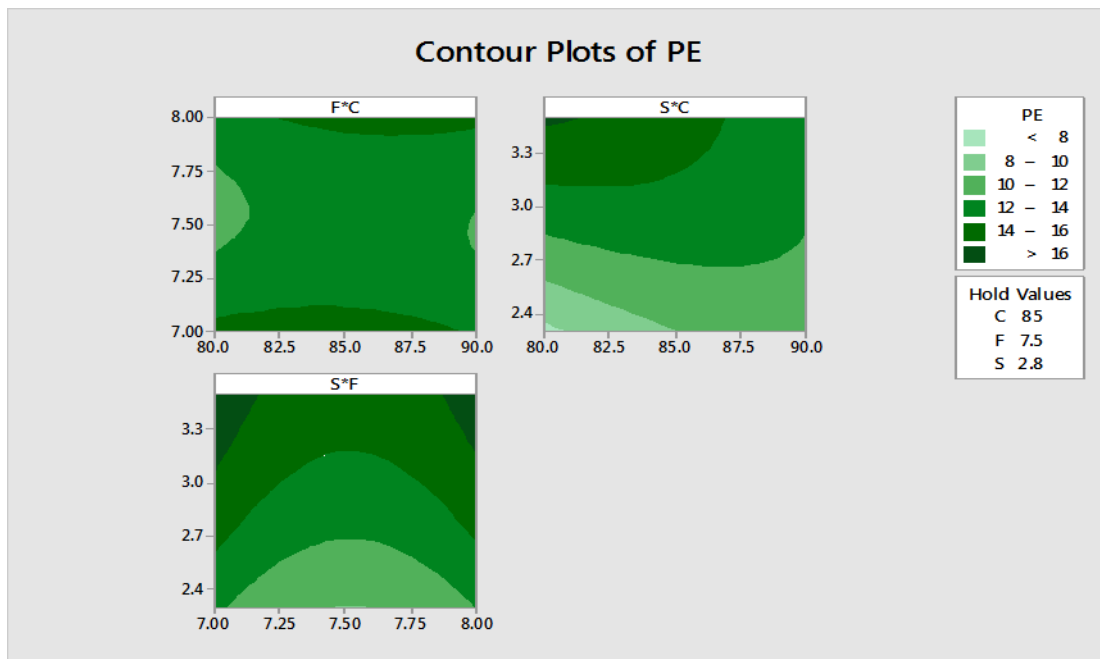


Figure 10. Contour plots of PE when welding current (C), gas flow rate (F) and speed of welding (S) constant at middle level

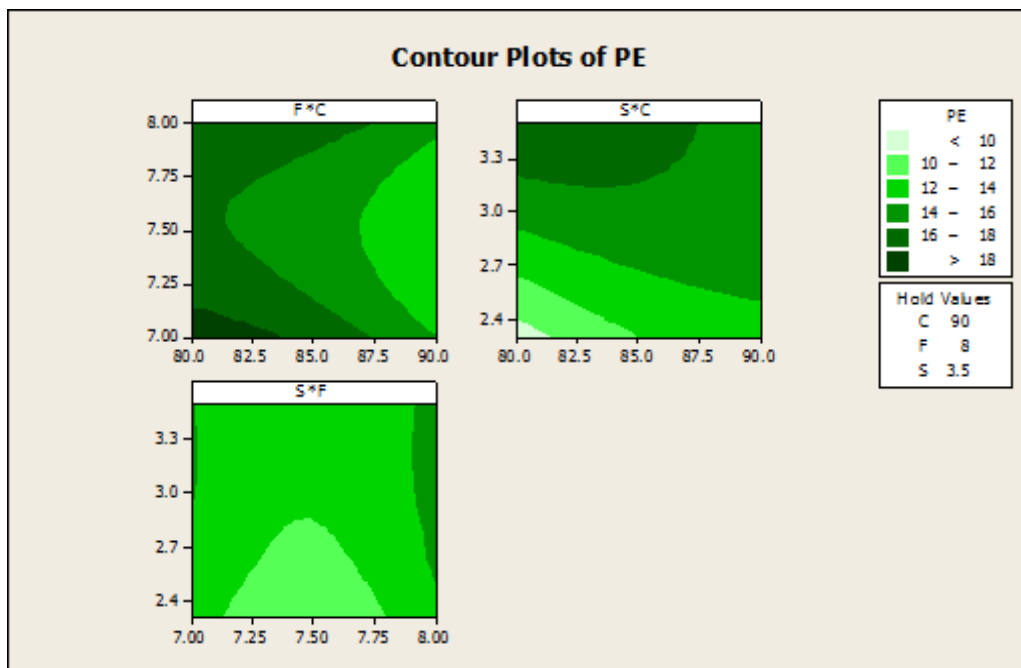


Figure 11. Contour plots of PE when welding current (C), gas flow rate (F) and speed of welding (S) constant at highest level

5. Conclusions

Based on the results of present investigation and analysis of the experimental data, the following conclusions are drawn in respect of TIG welding of duplex stainless-steel ASTM/UNS: 2205, of 3 mm thickness, within the range and the limit of the study:

1. Mathematical model for percentage of elongation has been prepared satisfactorily through non linear regression analysis.
2. Residual plots validate the regression model. From residual plots, it is clearly observed that

maximum data are satisfied and regression model is, therefore, considered valid.

3. Percentage deviation for PE is considered as acceptable. Figure 5 also indicates that the mathematical model works satisfactorily for the prediction of the response within the range of the experimental domain.
4. For surface plots, interaction among the welding factors, welding current (C) and gas flow rate (F) causes lesser influence on the response PE as compared to the interactions among the factors

gas flow rate (F), speed of welding (S) and welding current (C), speed of welding (S).

5. For contour plots, interaction among the factors welding current (C) and speed of welding (S) is found to be significant in so far as the effect of this interaction on PE is concerned. Interaction effect of welding current (C) and gas flow rate (F) on PE is not so much significant, as revealed in figures 9–11, while speed of welding (S) is kept in constant position.

References

- [1] N. Murugan, R.S. Paramar, S.K. Sud, Effect of submerged arc process variables on dilution and bead geometry in single wire surfacing, *Journal of Material Processing Technology*, 37 (1993) 767-780. [\[DOI\]](#)
- [2] R. Badji, M. Bouabdallah, B. Bacroix, C. Kahloun, B. Belkessa, H. Maza, Phase transformation and mechanical behavior in annealed 2205 duplex stainless steel welds, *Materials Characterization*, 59 (2008)447-453. [\[DOI\]](#)
- [3] M.E. Sotomayor, J. Sanz, A. Cervera, B. Levenfeld, A. Várez, Surface modification of a duplex stainless steel for plastic-metal hybrid parts, *Archives of Materials Science and Engineering*, 72 (2015) 86-93.
- [4] P.K. Palani, N. Murugan, Sensitivity Analysis for Process Parameters in Cladding of Stainless Steel by Flux Cored Arc Welding, *Journal of Manufacturing Processes*, 8 (2006) 90-100. [\[DOI\]](#)
- [5] J.J. Del Coz Diaz, P. M. Rodriguez, P.J. G. Nieto, D. Castro-Fresno, Comparative analysis of TIG welding distortions between austenitic and duplex stainless steels by FEM, *Journal of Applied Thermal Engineering*, 30 (2010) 2448-2459. [\[DOI\]](#)
- [6] S.N. Pandya, J.V. Menghani, Developments of mathematical models for prediction of tensile properties of dissimilar AA6061-T6 to Cu welds prepared by friction stir welding process using Zn interlayer, *Sadhana*, 43 (2018) 1-18. [\[DOI\]](#)
- [7] Y.S. Tarng, W.H. Yang, Optimisation of the weld bead geometry in gas tungsten arc welding by the Taguchi method, *The International Journal of advanced manufacturing technology*, 14 (198) 549-554. [\[DOI\]](#)
- [8] Y.S. Tarng, W.H. Yang, S.C. Juang, The use of fuzzy logic in the Taguchi method for the optimisation of the submerged arc welding process, *The International Journal of Advanced Manufacturing Technology*, 16 (2000) 688-694. [\[DOI\]](#)
- [9] Y.S. Tarng, S.C. Juang, C.H. Chang, The use of grey-based Taguchi methods to determine submerged arc welding process parameters in hard facing, *Journal of Materials Processing Technology* 128 (2002) 1-6. [\[DOI\]](#)
- [10] R.H. Murta, F.D. Braga, P.P. Maia, O.B. Diogenes, E.P. De Moura, Mathematical modeling for predicting mechanical properties in rebar manufacturing, *Ironmaking & Steelmaking*, 48 (2021) 161-169. [\[DOI\]](#)
- [11] R. Badjia, B. Bacroix, M. Bouabdallah, Texture, microstructure and anisotropic properties in annealed 2205 duplex stainless steel welds, *Journal of Materials Characterization*, 62 (2011) 833–843. [\[DOI\]](#)
- [12] Ul-Haq, H. Weiland, J.H. Bunge, Textures and microstructures in duplex stainless steel, *Materials Science and Technology*, 10 (1994) 289–298. [\[DOI\]](#)

Conflict of interest

The Authors have no conflicts of interest to declare that they are relevant to the content of this article.

Does this article screened for similarity?

Yes

About the License

© The Author(s) 2022. The text of this article is open access and licensed under a Creative Commons Attribution 4.0 International License.